

BiKT: Unleashing the potential of GNNs via Bi-directional Knowledge Transfer

Shuai Zheng, Zhizhe Liu, Zhenfeng Zhu*, Xingxing Zhang, Jianxin Li, *Member, IEEE*,
and Yao Zhao, *Fellow, IEEE*

Abstract—Based on the message-passing paradigm, there has been an amount of research proposing diverse and impressive feature propagation mechanisms to improve the performance of GNNs. However, less focus has been put on feature transformation, another major operation of the message-passing framework. In this paper, we first empirically investigate the performance of the feature transformation operation in several typical GNNs. Unexpectedly, we notice that GNNs do not completely free up the power of the inherent feature transformation operation. By this observation, we propose the **Bi-directional Knowledge Transfer (BiKT)**, a plug-and-play approach to unleash the potential of the feature transformation operations without modifying the original architecture. Taking the feature transformation operation as a derived representation learning model that shares parameters with the original GNN, the direct prediction by this model provides a topological-agnostic knowledge feedback that can further instruct the learning of GNN and the feature transformations therein. On this basis, BiKT not only allows us to acquire knowledge from both the GNN and its derived model but promotes each other by injecting the knowledge into the other. In addition, a theoretical analysis is further provided to demonstrate that BiKT improves the generalization bound of the GNNs from the perspective of domain adaption. An extensive group of experiments on up to 7 datasets with 5 typical GNNs demonstrates that BiKT brings up to 0.5% - 4% performance gain over the original GNN, which means a boosted GNN is obtained. Meanwhile, the derived model also shows a powerful performance to compete with or even surpass the original GNN, enabling us to flexibly apply it independently to some other specific downstream tasks.

Index Terms—Graph neural networks, knowledge transfer, feature transformation, domain adaption.



1 INTRODUCTION

THE advent of *Graph Neural Networks* (GNNs) has provided an attractive paradigm of representation learning for non-Euclidean data, especially graph data [1]. Benefiting from the universal ability to handle both node-level and graph-level tasks, there are many fields in which GNNs are being applied with impressing results, including recommendation [2], [3], chemistry analysis [4], [5], biomedicine [6], [7], and so on.

In general, the majority of existing GNNs are founded upon the message-passing framework, primarily comprising two core operations: feature propagation (**P**) and feature transformation (**T**). The **T** operation involves applying a nonlinear transformation to node representations, thereby serving to scale feature dimensions and enhance model capacity. On the other hand, the **P** operation is utilized for aggregating neighborhood representations into the target node's representation.

Within the message-passing framework, several approaches have emerged to enhance the capabilities of GNNs. These include attention mechanisms [8], multi-hop aggregation [9], [10], and novel processing pipelines [11], [12]. Most of these endeavors have concentrated on the **P** operation [8], [13], [14], [15], which is considered as the crucial element of GNNs to be able to handle non-Euclidean data effectively. Additionally, there have been general techniques aimed at improving the performance of the entire GNN family, from the perspective of regularization [16], [17] and training strategies [18], [19], rather than making specific modifications to individual models.

Undoubtedly, the aforementioned endeavors have significantly propelled the research and development of Graph Neural Networks (GNNs). Nevertheless, compared to the **P** operation, another pivotal facet within the message-passing framework, the **T** operation, garners relatively scant attention, with discussions primarily centering on feature dimension transformation and downstream tasks like classification. Specifically, when the **P** operation is excluded, and only the **T** operation is preserved, GNNs can be conceptualized as variations of *Multi-Layer Perceptrons (MLPs)* that apply multiple feature transformation operations along with a nonlinear activation function. Although MLPs are typically regarded as focusing solely on the node's features and thus have difficulty dealing with non-Euclidean data, recent studies show that MLPs can also gain the capability to rival GNNs in terms of graph learning with the support of some mechanisms, such as knowledge distillation [20], data augmentation [21], topological priors guidance [22], and so on [23]. When combining the inherent connection between

- S. Zheng, Z. Zhu, Z. Liu, and Y. Zhao are with the Institute of Information Science, Beijing Jiaotong University, Beijing 100044, China, and also with the Beijing Key Laboratory of Advanced Information Science and Network Technology, Beijing 100044, China. (E-mail: zs1997, zhzhzhu, zhzhliu, yzhao@bjtu.edu.cn.) Xingxing Zhang is with Qiyuan Lab, Beijing, China. (E-mail: xxzhang1993@gmail.com). Jianxin Li is with the Beijing Advanced Innovation Center for Big Data and Brain Computing, School of Computer Science and Engineering, Beihang University, Beijing 100083, China. (E-mail: lijx@act.buaa.edu.cn.)

This work was supported in part by Science and Technology Innovation 2030 - "New Generation Artificial Intelligence" Major Project under Grant No. 2018AAA0102101, and in part by the National Natural Science Foundation of China under Grants (No.61976018, No.U1936212, No.62120106009).

*Corresponding author: Zhenfeng Zhu.

Manuscript received April 19, 2005; revised August 26, 2015.

MLPs and the **T** operation within GNNs, it obviously provokes an intriguing question for contemplation: **(Q1)** *Has the feature transformation within GNNs truly reached its full potential?* Furthermore, given that various adaptations of the **P** operation have yielded performance improvements for GNNs as a whole, it naturally leads to the question: **(Q2)** *Is the feature transformation within GNNs also influenced by feature propagation?* In light of these two thought-provoking questions, arises the subsequent inquiry: **(Q3)** *How can GNNs be further enhanced through the effective utilization of the feature transformation operation?*

To provide some insights into **(Q1)** and **(Q2)**, in this paper, we first perform an empirical analysis of the performance of GNNs with and without **P** operations to investigate the role of **T** operations in GNNs, as well as the interactive effects between **T** operations and **P** operations. The findings indicate that the structural bias introduced through explicit application of the **P** operation to the graph’s topology does indeed influence the representation modeling performed by the **T** operation for node content features. Furthermore, it becomes evident that GNNs have not harnessed the full potential of their **T** operations for feature representation modeling.

Building upon these insightful observations, we propose the **Bi-directional Knowledge Transfer** to address **(Q3)**, abbreviated as **BiKT** in this paper. It presents a versatile and adaptable solution to unleash the latent potential residing within the **T** operations of GNNs, to further enhance the performance of GNNs. It’s essential to emphasize that **BiKT** enhances GNNs without requiring any modifications to the original GNN architecture.

Let an instantiated GNN as the host GNN. By preserving only the **T** operation, the host GNN can derive a structure-independent MLP-like model that shares parameters with the host GNN. To integrate the feature modeling capacity of the derived model and the structural inductive bias inherent in the host GNN, **BiKT** gains the model knowledge by capturing the representation distributions of two models through two generators. Then, we achieve bi-directional knowledge transfer between the host GNN and the derived model, thereby fully unleashing the potentials of **P** and **T** in the host GNN. More importantly, we prove that the proposed **BiKT** improves the generalization bound of the host GNN to support the effectiveness of **BiKT**.

A comprehensive set of experiments conducted on diverse real-world datasets, varying in scale and properties, confirms that **BiKT** can significantly enhance existing GNNs. Moreover, the derived model also gains the ability to compete with or even surpass the original host GNN through **BiKT**. Therefore, **BiKT** allows us to choose whether to employ the derived model for fast inference or the host GNN with high accuracy, depending on the demand of downstream tasks and scenarios. In summary, the main contributions of this paper can be highlighted as follows:

- Rather than concentrating solely on the feature propagation operation, as seen in prior research, we redirect our focus to the feature transformation operation within GNNs and highlight that it has not been optimally harnessed within current frameworks.
- To fully leverage the capabilities of the feature trans-

formation, the **Bi-directional Knowledge Transfer (BiKT)** as a universal approach is proposed to facilitate knowledge transfer between the host GNN and the derived model built using feature transformation operations stripped from the host GNN.

- We conduct a theoretical analysis of the optimization objective introduced in **BiKT** and illustrate its impact on the generalization capabilities of GNNs.
- With five typical GNNs, our experiments demonstrate that **BiKT** can significantly enhance the performance of GNNs and their corresponding derived models in two tasks across several datasets.

2 PRELIMINARIES

Notations. An undirected graph with n nodes can be denoted as $\mathcal{G} = (\mathcal{V}, \mathcal{E})$, where \mathcal{V} represents the node set with $|\mathcal{V}| = n$ and \mathcal{E} represents the set of edges among nodes. Generally, the adjacency matrix $\mathbf{A} \in \mathbb{R}^{n \times n}$ is used to describe the topological structure of \mathcal{G} where $\mathbf{A}_{i,j} = 1$ if $(i, j) \in \mathcal{E}$ else 0. We assume that each node $u \in \mathcal{V}$ has associated with a corresponding d -dimensional feature vector $\mathbf{x}_u \in \mathbb{R}^d$, which can stack up to the feature matrix $\mathbf{X} \in \mathbb{R}^{n \times d}$. For the node classification task, there is a set of class labels $\mathcal{Y} = \{1, \dots, C\}$ with $|\mathcal{Y}| = C$ and each node $u \in \mathcal{V}$ is assigned a label $y_u \in \mathcal{Y}$, where C is the number of class. In addition, we adopt $\mathbf{y}_u \in \mathbb{R}^C$ to denote the one-hot vector corresponding to y_u . The problem is that the model needs to give the predicted result $\hat{\mathbf{y}}_u$ for a node.

Graph Neural Networks. The vast majority of GNN is built on the message-passing paradigm [8], [24], [25]. Although several GNNs are proposed from the perspective of the spectral domain, they can still be formulated in the message-passing paradigm, such as GCN [26] and FAGCN [14]. Intuitively, the basic form of the message-passing paradigm can be summarized as follows. First, the representations of neighbor nodes are propagated into the representations of the target node. Then, the representation of the target node is updated by a nonlinear transformation. Considering a L -layer GNN built on the message-passing paradigm, whose each layer can be decomposed into two operations, i.e., the feature propagation operation (**P**) and the feature transformation operation (**T**):

$$(\mathbf{P}) : \tilde{\mathbf{Z}}^{(l-1)} = \phi^{(l)}(\mathbf{Z}^{(l-1)}, \mathbf{A}), \quad (\mathbf{T}) : \mathbf{Z}^{(l)} = \psi^{(l)}(\tilde{\mathbf{Z}}^{(l-1)}). \quad (1)$$

where $\mathbf{Z}^{(l)}$ denotes the node representation matrix obtained at the l -th layer and $\mathbf{Z}^{(0)} = \mathbf{X}$ as the initial representation matrix, $\phi^{(l)}$ and $\psi^{(l)}$ are the message function and transformation function at the l -th layer, respectively. For the node classification task, the final representation $\mathbf{z}_u^{(L)}$ for a specific node u can be obtained after L layers. For different GNNs, some models use an additional linear inference layer as the classifier to obtain $\hat{\mathbf{y}}_u$, while others directly use the **T** operation of the L -th layer as the classifier. In the following sections, we use the latter as an example for the methodological discussion, but the proposed method can also apply to the former as well.

Taking GCN [26] as an example, the non-parametric weighted summation function based on \mathbf{A} is adopted as

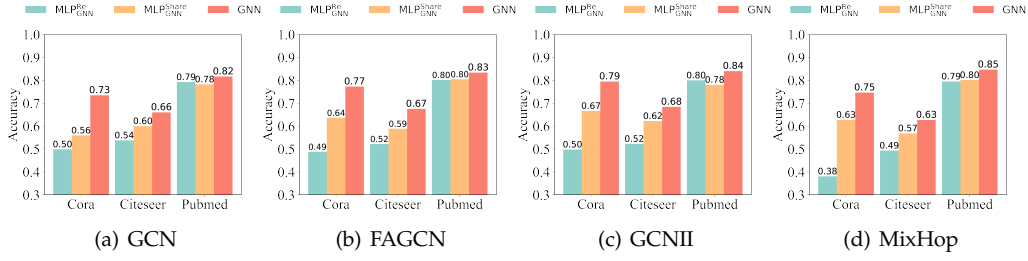


Fig. 1. Performance comparison of the GNN, MLP_{GNN}^{Re} , and MLP_{GNN}^{Share} with different GNN architectures, where MLP_{GNN}^{Re} denotes the re-initialized and trained MLP_{GNN} , and MLP_{GNN}^{Share} denotes the MLP_{GNN} that directly adopts the parameters of trained GNN for inference.

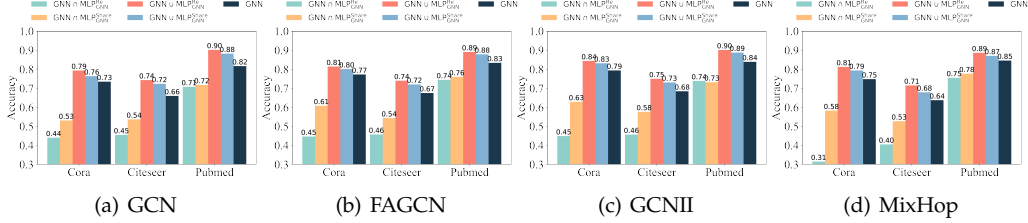


Fig. 2. Results of the union $GNN \cup MLP_{GNN}$ and intersection $GNN \cap MLP_{GNN}$ of the correct prediction sets of GNN and MLP_{GNN} .

TABLE 1

The performance of GCN and MLP_{GCN}^{Re} on assortative and disassortative nodes, respectively. BiKT-GCN obtains a considerable performance gain over GCN on disassortative nodes. The results demonstrate the effectiveness of BiKT in terms of combining the advantages of MLP_{GCN} and feature propagation in dealing with assortative and disassortative nodes.

Dataset	Eval	MLP_{GCN}^{Re}	GCN	BiKT-GCN
Cora	Assort.	54.59±3.12	75.45±5.30	85.08±3.73
	Disassort.	35.68±3.44	31.07±3.76	37.50±3.00
Citeseer	Assort.	55.87±4.56	65.62±5.78	70.42±2.66
	Disassort.	59.53±4.34	52.33±4.11	65.14±3.20
Pubmed	Assort.	84.94±1.10	92.43±0.66	93.20±0.77
	Disassort.	61.87±2.00	35.91±1.41	40.42±1.13

ϕ , and ψ is set as the fully-connected layer with non-linear activation. If we set the adjacency matrix \mathbf{A} as an identity matrix \mathbf{I}_n , we can notice that the GNN will degrade to a structure-independent MLP-like network, consisting solely of \mathbf{T} operations within the GNN. This transformation is akin to eliminating all \mathbf{P} operations in the GNN.

In this work, we define the GNN as the host GNN and the corresponding derived MLP-like network as MLP_{GNN} .

3 EMPIRICAL INVESTIGATION

To delve into the exploration of (Q1) and (Q2), as introduced in Section 1, we present an empirical yet insightful case study designed to assess whether GNNs fully harness the potential of \mathbf{P} operations. The core concept behind this study is to evaluate the performance disparities and examine the congruence of correctly predicted outcomes between the host GNN and MLP_{GNN} . The host GNN can be regarded as effectively leveraging \mathbf{T} operations if the correct predictions made by MLP_{GNN} are also reflected in the correct prediction outcomes of the GNN. Conversely, if the GNN fails to preserve the correct results predicted by MLP_{GNN} , it suggests that there is room for improvement in GNN, as it has not yet fully exploited the correct predictive capabilities exhibited by MLP_{GNN} .

Setup. To ensure the generalizability of the experimental results, we selected 4 typical GNNs for validation. The node classification experiment is conducted on 3 widely used citation networks: Cora, Citeseer, and Pubmed [27]. We also calculate the homophily ratio $h(v)$ for each node according to [28] and select the nodes with $h(v) < 0.2$ as disassortative nodes and $h(v) > 0.8$ as assortative nodes. To comprehensively verify the performance of \mathbf{T} operations in GNNs, the following two cases are set up for MLP_{GNN} :

- 1). After completing the standard training of the GNN, during the testing phase, we first convert the GNN into MLP_{GNN} by replacing the adjacency matrix \mathbf{A} with the identity matrix \mathbf{I} , and subsequently employ this MLP_{GNN} for inference. This MLP_{GNN} is denoted as MLP_{GNN}^{Share} since it directly adopts the trained parameters of the host GNN.
- 2). We directly convert the untrained GNN to MLP_{GNN} by replacing the adjacency matrix \mathbf{A} with the identity matrix \mathbf{I} , and then we directly train this MLP_{GNN} for node classification. This scheme is denoted by MLP_{GNN}^{Re} .

We run the experiment 10 times with random seeds and report the average accuracy of GNN, MLP_{GNN}^{Share} , and MLP_{GNN}^{Re} . Besides, we take the union $GNN \cup MLP_{GNN}$ and intersection $GNN \cap MLP_{GNN}$ of the correct prediction sets of GNN and MLP_{GNN} respectively, and report the accuracy of the union set and interaction set.

Result Analysis. As shown in Fig. 1, regardless of the architecture of GNNs, both MLP_{GNN}^{Share} and MLP_{GNN}^{Re} exhibit inferior performance compared to the corresponding GNN. It demonstrates that the effective utilization of topology is one of the keys to the excellent performance of GNN, which is also consistent with the findings of previous studies [12], [18]. Meanwhile, it also should be noticed that MLP_{GNN}^{Share} outperforms MLP_{GNN}^{Re} on the Cora and Citeseer datasets and $GNN \cap MLP_{GNN}^{Share}$ improves significantly compared to $GNN \cap MLP_{GNN}^{Re}$. It shows that the explicit structural bias brought by \mathbf{P} operations may benefit MLP_{GNN} to capture the structural information to some extent.

Besides, as shown in Table 1, while \mathbf{P} facilitates the classification of assortative nodes for GNN, it also leads to difficulties in dealing with disassortative nodes. On the

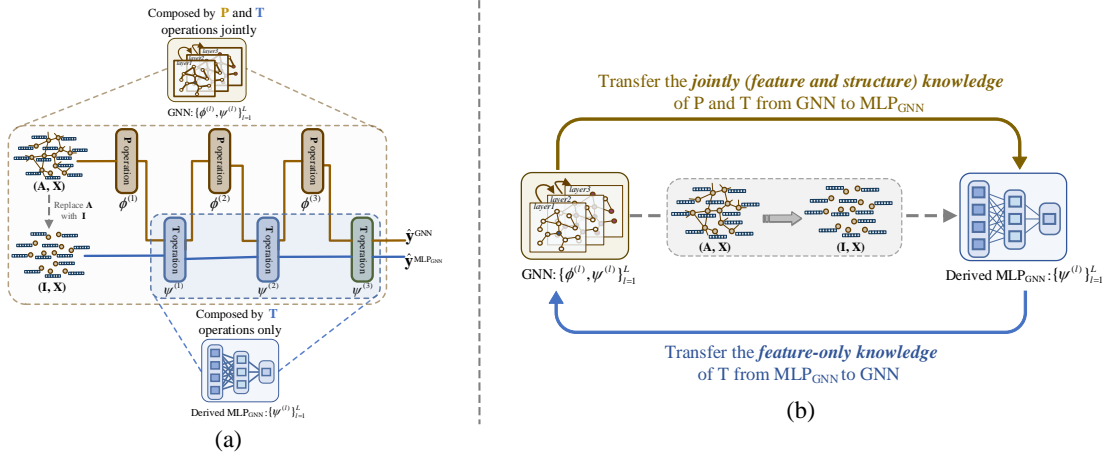


Fig. 3. The motivation of BiKT. (a) illustrates the relationship between the GNN and the derived MLP_{GNN} and (b) shows the knowledge transfer between two models. The **P** operations in GNN introduce a strong relation inductive bias into the representation modeling of **T** operations, influencing the focus of the feature transformation on the node features. Bi-directional knowledge transfer between GNN and MLP_{GNN} will allow us to achieve a better trade-off between node features and structural biases, leading to more effective node representation.

contrary, when dealing with those disassortative nodes, MLP_{GNN}^{Re} without using any structural prior shows a more powerful ability than GNN.

More importantly, as we can observe from Fig. 2, $\text{GNN} \cup \text{MLP}_{\text{GNN}}^{\text{Re}}$ shows the best performance on each dataset whatever the GNN is used. $\text{GNN} \cup \text{MLP}_{\text{GNN}}^{\text{Re}}$ can outperform the GNN by about 5%-10%, which demonstrates that MLP_{GNN}^{Re} captures some beneficial information that the GNN cannot grasp from the node content feature, despite the poor performance of MLP_{GNN}^{Re}. Besides, although $\text{GNN} \cup \text{MLP}_{\text{GNN}}^{\text{Share}}$ declines slightly compared to $\text{GNN} \cup \text{MLP}_{\text{GNN}}^{\text{Re}}$, it still outperforms the GNN by a considerable amount. This indicates that the **P** operation is also unable to help the host GNN retain the specific knowledge obtained by MLP_{GNN} from node features.

Summary. The empirical investigation mentioned above can roughly provide an answer for (Q1) that GNN does not unleash the full potential of **T** operations no matter what the architecture of the GNN is, since the GNN throws away the valuable information already captured by **T** operations from node content feature. In addition, this case study also hints at an interesting observation for (Q2) that **P** operations could inject some knowledge about the topological structure of the graph from the host GNN into MLP_{GNN} to strengthen its capability. On the contrary, **P** operations cannot realize the knowledge transfer from MLP_{GNN} to the GNN as a whole. Furthermore, the **P** operation inherently introduces a strong relational induction bias in the representation learning process, as pointed out in [29]. It brings GNN the ability which generally cope well with assortative nodes containing strong structural relationships. As a model that is perceived as having no or very little inductive bias [29], MLP can perform representation learning by relying only on the raw features of nodes in the absence of structural prior. It means that the **T**-only training for MLP_{GNN} can be favorably served as a complementary of **P** operation of the host GNN, allowing us to achieve a better trade-off between node feature modeling and structural biases.

4 BI-DIRECTIONAL KNOWLEDGE TRANSFER

As illustrated in Fig. 3, The observations mentioned above motivate us to seek a mechanism to achieve the mutual knowledge transfer between the GNN and MLP_{GNN}, thereby seamlessly combining the advantages of feature transformation and feature propagation in aspects of feature modeling and structural inductive bias.

For this purpose, rather than introducing a new GNN by meticulously altering the model architecture, the proposed Bi-directional Knowledge Transfer (BiKT) accomplishes knowledge capture from both the GNN and MLP_{GNN} by modeling their representation distributions, and then progressively infuses the knowledge into each other.

4.1 Generation-based Representation Distribution Modeling

Not limited to model parameters, a broader view of model knowledge is a learned mapping from input to output [30]. Considering the structural bias introduced by **P** in GNN during representation learning, to capture the model knowledge from GNNs and MLP_{GNN}, we utilize the representation distribution of the model as a surrogate for the learned model mapping to instantiate the model knowledge.

In particular, let $\mathcal{X} \subset \mathbb{R}^d$ be the raw feature space and $\mathcal{Z} \subset \mathbb{R}^{d_m}$ be the representation space. For a L -layer GNN, it can be separated into two components: a feature extractor $f_{\text{gnn}}(\mathbf{X}, \mathbf{A}) : \mathcal{X} \rightarrow \mathcal{Z}$ composed by all operations except for $\psi^{(L)}$, and a classifier $f_{\text{cls}}(\mathbf{Z}) : \mathcal{Z} \rightarrow \mathcal{Y}$ played by $\psi^{(L)}$. Similarly, MLP_{GNN} can also be separated as: $f_{\text{mlp}}(\mathbf{X})$ composed by $\{\psi^{(l)}\}_{l=1}^{L-1}$, and $f_{\text{cls}}(\mathbf{Z})$. Due to the explicit involvement of **A** in the representation learning process, the representation distribution modeled by **T** operations has been altered by additional **P** operations. It not only injects the information of topological structure into the representation distribution but also interferes with the knowledge from content features. It means the representation distribution from f_{gnn} can be seen that embed the joint knowledge of structural information and node features, while the representation distribution from f_{mlp} captures knowledge only from node features.

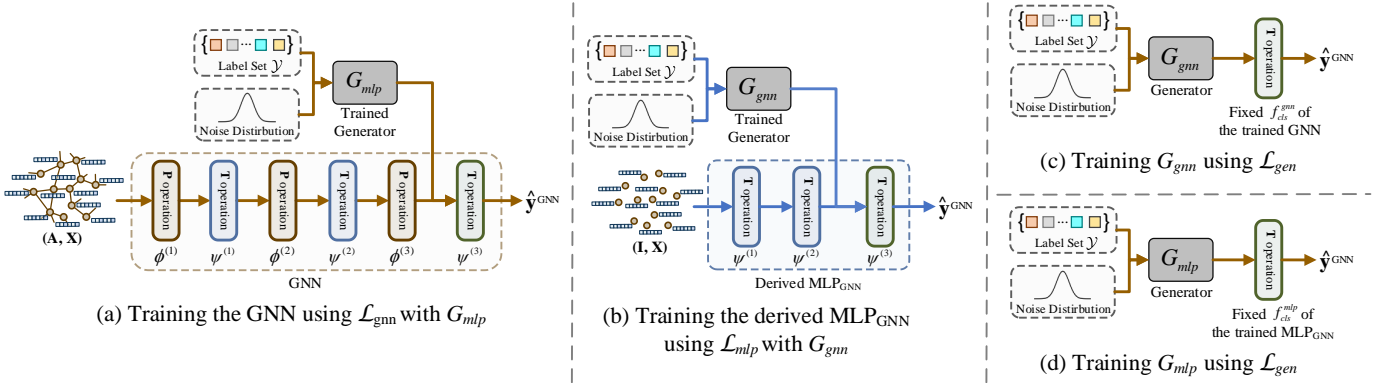


Fig. 4. An overview of BiKT to show the parts of the training involved in each phase. During the recurrent training, (a)(c) and (b)(d) would be performed alternately to establish the bi-directional knowledge transfer between GNN and MLP_{GNN} .

To achieve the representation distribution modeling effectively, we consider learning an auxiliary conditional distribution $q(\mathbf{z}|y) : \mathcal{Y} \rightarrow \mathcal{Z}$. It is applied to fit the representation distribution extracted by the given model, thus back-capturing the knowledge embedded in the representation distribution. Let $p(y|\mathbf{z})$ be the learned posterior distribution of the model and $p(y)$ be the ground-truth prior distribution of labels, $q(\mathbf{z}|y)$ can be modeled as:

$$q(\mathbf{z}|y) = \arg \max_{q(\mathbf{z}|y)} H(q(\mathbf{z}|y)) + \mathbb{E}_{y \sim p(y)} \mathbb{E}_{\mathbf{z} \sim q(\mathbf{z}|y)} [\log p(y|\mathbf{z})] \quad (2)$$

where $H(q(\mathbf{z}|y))$ denotes the entropy of $q(\mathbf{z}|y)$, which is used to ensure the diversity of \mathbf{z} .

Specifically, we adopt the uniform distribution $\hat{p}(y)$ as an alternative to $p(y)$, since not all nodes' labels are available and therefore $p(y)$ is unknown during the training phase. The counting of the observable labels in the training set is also a common practice to approximate $p(y)$. Further, inspired by the idea of generative models [31], [32], [33], a conditional generator G is adopted to learn $q(\mathbf{z}|y)$ as $G(y, \varepsilon | \varepsilon \sim \mathcal{N}(0, \mathbf{I}_{d_m}))$, where ε is a noise vector sampled from d_m -dimensional standard normal distribution. Since we rely on the generator G to realize the non-parametric estimation of $q(\mathbf{z}|y)$, it is not easy to calculate $H(q(\mathbf{z}|y))$ directly. To bypass this problem, the mode-seeking regularization term $D(G)$ from [34] is adopted as a substitute for $H(q(\mathbf{z}|y))$ to escort the diversity of \mathbf{z} :

$$D(G) = \max_G \mathbb{E}_{y \sim \hat{p}(y)} \mathbb{E}_{\varepsilon_1, \varepsilon_2 \sim \mathcal{N}(0, \mathbf{I}_{d_m})} \left[\frac{d_{\mathbf{z}}(G(y, \varepsilon_1), G(y, \varepsilon_2))}{d_{\varepsilon}(\varepsilon_1, \varepsilon_2)} \right] \quad (3)$$

where $d_*(\cdot)$ denotes the distance metric. According to Eq. (2) and Eq. (3), the generator G can be trained to model $q(\mathbf{z}|y)$ through minimizing the following optimization objective:

$$\mathcal{L}_{gen} = \mathbb{E}_{y \sim \hat{p}(y)} \mathbb{E}_{\varepsilon \sim \mathcal{N}(0, \mathbf{I}_{d_m})} [\mathcal{L}_{sl}(\sigma(f_{cls}(G(y, \varepsilon))), y)] - D(G) \quad (4)$$

where \mathcal{L}_{sl} and σ are the classification loss function and the activation function, respectively. It can be seen that we only need the classifier f_{cls} to participate in the modeling of $q(\mathbf{z}|y)$, which is an efficient practice to capture the knowledge of models.

According to the generator learning mentioned above, BiKT could acquire model knowledge from both the host GNN and the derived MLP_{GNN} by fitting the representation distributions captured from them according to the two generators as shown in Fig. 4(c) and (d), respectively.

4.2 Knowledge Infusion

To achieve knowledge transfer between the GNN and MLP_{GNN} , we need to address how to inject knowledge gained from one model (target model) into the other model (source model).

To this end, we incorporate the generator G_{tgt} into the training process of the source model as a regularizer, which has been trained to model the distribution $q_{tgt}(\mathbf{z}|y)$ of the target model according to Eq. (4). It means that the source model will be subject to two key constraints during the optimization process: the direct supervised loss from the downstream task, and the knowledge infusion loss from the generator. To be specific, given a label set $\{\tilde{y}_i\}_{i=1}^K$ that sampled from $p(y)$, the corresponding representation set $\tilde{\mathbf{Z}}_{tgt} = \{\tilde{\mathbf{z}}_i\}_{i=1}^K$ can be sampled from $q_{tgt}(\mathbf{z}|y)$ by G_{tgt} . Consequently, for the source model, the knowledge infusion regularization term can be formulated as:

$$\mathcal{L}_{ki}(\tilde{\mathbf{Z}}_{tgt}, f_{cls}^{tgt}) = \sum_{\tilde{\mathbf{z}}_i \in \tilde{\mathbf{Z}}_{tgt}} \mathcal{L}_{sl}(\sigma(f_{cls}^{tgt}(\tilde{\mathbf{z}}_i)), \tilde{y}_i) \quad (5)$$

where \mathcal{L}_{sl} denotes the supervised loss, for the node classification task, we employ the cross-entropy loss as \mathcal{L}_{sl} .

According to Eq. (5), the generators can be involved in the training procedure of each model. Concretely, when GNN serves as the source model and MLP_{GNN} as the target model, GNN can integrate the knowledge from MLP_{GNN} with the assistance of G_{mlp} by minimizing the following optimization objective:

$$\mathcal{L}_{gnn} = \sum_{u \in \mathcal{V}^{trn}} \mathcal{L}_{sl}(\hat{y}_u^{gnn}, y_u) + \alpha \mathcal{L}_{ki}(\tilde{\mathbf{Z}}_{mlp}, f_{cls}^{mlp}) \quad (6)$$

where \mathcal{V}^{trn} denotes the set of training nodes, \hat{y}_u^{gnn} denotes the predicted probability vector for node u by the GNN, and α is a coefficient to control the strength of \mathcal{L}_{ki} .

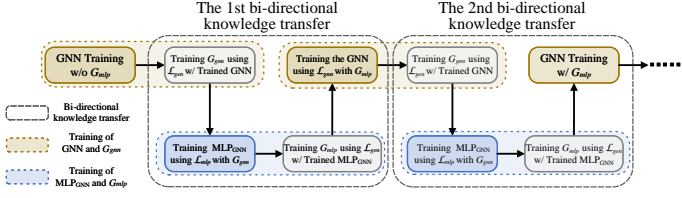


Fig. 5. The illustration of the recurrent training with parameter inheritance between MLP_{GNN} and GNN. This practice facilitates the progressive knowledge integration of both sides.

On the contrary, when MLP_{GNN} serves as the source model and GNN as the target model, the total loss function for MLP_{GNN} through BiKT can be formulated as:

$$\mathcal{L}_{mlp} = \sum_{u \in \mathcal{V}^{trn}} \mathcal{L}_{sl}(\hat{\mathbf{y}}_u^{mlp}, y_u) + \alpha \mathcal{L}_{ki}(\tilde{\mathbf{Z}}_{gnn}, f_{cls}^{gnn}) + \beta \mathcal{L}_{ps}(\hat{\mathbf{Y}}_{\mathcal{V}}^{mlp}, \hat{\mathbf{Y}}_{\mathcal{V}}^{gnn}) \quad (7)$$

where $\hat{\mathbf{y}}_u^{mlp}$ denotes the predicted probability vector for node u by MLP_{GNN} and the KL-divergence is used to serve as \mathcal{L}_{ps} . Besides, $\hat{\mathbf{Y}}_{\mathcal{V}}^* = \{\hat{\mathbf{y}}_u^*\}_{u \in \mathcal{V}}$ denotes the set of the predicted probability vector for \mathcal{V} , $\hat{\mathbf{Y}}_{\mathcal{V}}^{mlp}$ and $\hat{\mathbf{Y}}_{\mathcal{V}}^{gnn}$ is the sets corresponding to MLP_{GNN} and GNN respectively, β is also a coefficient to control the strength of \mathcal{L}_{ps} .

Compared to Eq. (6) for GNN, it can be observed from Eq. (7) includes an additional term \mathcal{L}_{ps} . This regularization term is introduced to reduce the huge gap in performance between MLP_{GNN} and GNN at the initial stage. \mathcal{L}_{ps} utilizes the predictions of GNN as reliable results to guide the training of MLP_{GNN} . This provides a direct and efficient method for transferring structural information from GNN to MLP_{GNN} , complementing the indirect distribution-level knowledge infusion through G_{gnn} .

4.3 Progressive Knowledge Transfer with Parameter Inheritance

Generally speaking, a one-way knowledge transfer from MLP_{GNN} to the host GNN can achieve the goal of enhancing \mathbf{T} within GNN. However, such a practice only allows the host GNN to benefit from the initial MLP_{GNN} , not from the optimized MLP_{GNN} according to Eq. (7). Moreover, \mathbf{T} still relies on \mathbf{P} to explicitly inject structural bias and cannot autonomously learn this inductive bias by itself. Inspired by the concept of continuous learning [35], we adopt a recurrent training strategy between MLP_{GNN} and GNN to integrate knowledge from both sides progressively.

To be specific, the host GNN and MLP_{GNN} are trained alternately in the form of recurrent training with parameter inheritance, as shown in Fig. 5. The model parameter is a foundational form of model knowledge [30], which can be shared directly between models of the same architecture to enable knowledge inheritance. Moreover, it can be observed from Section 3 that the parameters of a properly trained GNN provide a favorable initialization for MLP_{GNN} compared to a random initialization. Hence, for the host GNN and the derived MLP_{GNN} , after either model completes the training procedure, its model parameters are directly inherited by the other model as model initialization. This strategy not only facilitates knowledge transfer between

models, but also alleviates knowledge forgetting that may occur during training.

Based on the parameter inheritance, the host GNN and MLP_{GNN} can be trained alternately based on each other's parameter knowledge. We alternate the roles of the host GNN and MLP_{GNN} as the source model and the target model during the recurrent training process to establish bi-directional knowledge transfer. This process shares a fascinating similarity indeed with the classical co-training paradigm [36]. In practice, we first perform a standard training of the host GNN to obtain a base model according to Eq. (6) with $\alpha = 0$. Then, a complete bi-directional knowledge transfer between the host GNN and the derived MLP_{GNN} can be described as follows: Based on the trained f_{cls}^{gnn} in the host GNN, a generator G_{gnn} is instantiated to model $q_{gnn}(\mathbf{z}|y)$ according to Eq. (4). Next, according to Eq. (7) and G_{gnn} , we proceed with the further training of the MLP_{GNN} which inherits parameters from the host GNN. After the training of MLP_{GNN} , G_{mlp} is used to learn $q_{mlp}(\mathbf{z}|y)$. Similarly, in the next training phase of the host GNN, G_{mlp} can play a vital role in seamlessly integrating the knowledge, which exclusively stems from node features via MLP_{GNN} , into the host GNN according to Eq. (6). The process can be executed recurrently several times according to the parameter inheritance mechanism.

4.4 Generalization Analysis of BiKT

The core idea of BiKT is to extract model knowledge from the host GNN and the derived MLP_{GNN} by modeling the representation distribution $q_{gnn}(\mathbf{z}|y)$ and $q_{mlp}(\mathbf{z}|y)$ and then integrating the distribution into the learning process of each other to achieve knowledge transfer. As a result, *whether the generator can successfully fit the induced distribution of the target model from \mathcal{Y} to \mathcal{Z}* plays a crucial role in the feasibility of BiKT. To dispel such doubt, we have the following proposition:

Proposition 4.1. *Let $q(\mathbf{z}|y)$ be the distribution modeled by generator G , $p(y|\mathbf{z}; f_{cls})$ and $p(\mathbf{z}|y; f_{cls})$ be the posterior distribution and the corresponding induce distribution of f_{cls} . Then maximizing Eq. (2) is equivalent to minimizing the conditional KL-divergence between $q(\mathbf{z}|y)$ and $p(\mathbf{z}|y; f_{cls})$.*

For proof of **Proposition 4.1**, please refer to the Appendix A.

By showing the connection between the optimization objective of the generator and the conditional KL-divergence between $q(\mathbf{z}|y)$ and $p(\mathbf{z}|y; f_{cls})$, **Proposition 4.1** demonstrates that generator could fit the induced distribution of the target model based on the optimization objective.

Moreover, as we mentioned in Sect. 2, the host GNN is equivalent to MLP_{GNN} in the case where \mathbf{A} is set to an identity matrix \mathbf{I}_n . Therefore, by treating the node features \mathbf{X} and topological structure \mathbf{A} as a whole set, we could define the distributions of set (\mathbf{X}, \mathbf{A}) and $(\mathbf{X}, \mathbf{I}_n)$ as \mathcal{D}_{gra} and \mathcal{D}_{fea} respectively. Following the definition provided in [37], we can view the distributions \mathcal{D}_{gra} and \mathcal{D}_{fea} as two distinct domains. The problem addressed in this paper can thus be framed as a domain adaptation problem. To elaborate, once we have completed the training of the host GNN, evaluating the performance of the $\text{MLP}_{\text{GNN}}^{Share}$ is equivalent to assessing the impact of transferring the model

to the \mathcal{D}_{fea} domain after training in \mathcal{D}_{gra} . Therefore, we can analyze *whether the source model can benefit from the captured distribution of the generator* from the perspective of domain adaption. We first let the distribution $q(\mathbf{z}|y)$ derived by the generator satisfy the following assumption after optimization according to **Proposition 4.1**:

Assumption 4.1. Given f_{cls}^{tgt} and f_{cls}^{src} of the target model and source model respectively, $q(\mathbf{z}|y)$ approximate $p(\mathbf{z}|y; f_{cls}^{tag})$ and have $d_{\mathcal{H}}(q(\mathbf{z}|y), p(\mathbf{z}|y; f_{cls}^{tag})) \leq d_{\mathcal{H}}(p(\mathbf{z}|y; f_{cls}^{src}), p(\mathbf{z}|y; f_{cls}^{tag}))$, where $d_{\mathcal{H}}$ denotes the \mathcal{H} -divergence.

Then, based on the generalization bound for domain adaption proposed in [37], [38], we have:

Proposition 4.2. Suppose assumption 1 holds. Let \mathcal{T} and \mathcal{S} be the source domain and target domain with the distribution \mathcal{D}_s and \mathcal{D}_t , respectively. Let \mathcal{R} be a representation function from \mathcal{X} to \mathcal{Z} . Denote \mathcal{D}_G be an auxiliary distribution derived from a generator G and $\mathcal{D}'_s = \tau\mathcal{D}_G + (1 - \tau)\mathcal{D}_s$. Denote \mathcal{H} be a set of hypothesis with VC-dimension d . Given an empirical dataset $\hat{\mathcal{D}}_s$ and an augmented dataset $\hat{\mathcal{D}}'_s$ with $|\hat{\mathcal{D}}_s| = m$ and $|\hat{\mathcal{D}}'_s| = m' > m$. Let $J(m, d) = \sqrt{\frac{4}{m} (d \log \frac{2em}{d} + \log \frac{4}{\delta})}$, where e is the base of the natural logarithm. If $(\epsilon_{\mathcal{S}}(h) - \epsilon_{\mathcal{S}'}(h))$ is bounded and $m > \frac{1}{2}d$, then with probability at least $1 - \delta$, for every hypothesis $h \in \mathcal{H}$:

$$\begin{aligned} \epsilon_{\mathcal{T}}(h) &\leq \hat{\epsilon}_{\mathcal{S}'}(h) + J(m', d) + d_{\mathcal{H}}(\hat{\mathcal{D}}'_s, \tilde{\mathcal{D}}_t) + \lambda' \\ &\leq \hat{\epsilon}_{\mathcal{S}}(h) + J(m, d) + d_{\mathcal{H}}(\tilde{\mathcal{D}}_s, \tilde{\mathcal{D}}_t) + \lambda \end{aligned} \quad (8)$$

where $\epsilon_*(h)$ and $\hat{\epsilon}_*(h)$ are the expected and empirical risk of h on the domain respectively. \mathcal{S}' denotes the augmented source domain with $\tilde{\mathcal{D}}'_s$, $\lambda = \min_h (\epsilon_{\mathcal{T}}(h) + \epsilon_{\mathcal{S}}(h))$ and $\lambda' = \min_h (\epsilon_{\mathcal{T}}(h) + \epsilon_{\mathcal{S}'}(h))$ is the optimal risk on two domains.

For proof of **Proposition 4.2**, please refer to the Appendix A.

As we can see from **Proposition 4.2**, the generated distribution by G could improve the generalization performance of the model trained in the source domain when applied to the target domain. It means the generator could facilitate the host GNN and MLP_{GNN} to adapt to each other's distribution, i.e., achieving the knowledge transfer between the two models.

Complexity Analysis of BiKT. Since no additional computational units are introduced for the GNN and MLP_{GNN} , there is no extra computational complexity introduced in one training phase of the GNN and MLP_{GNN} . The main computational overhead of BiKT comes from multiple iterative training. Due to the fact that the computational complexity of the GNN and MLP varies depending on the specific GNN used, let's denote the computational complexity of GNN to be $O(O_{gmn})$ and the computational complexity of MLP and generators to be $O(O_{mlp})$. Then the computational complexity of BiKT during training can be roughly expressed as $O(tO_{mlp} + 3tO_{gmn})$, where t is the number of iterations.

Take GCN as an example, let n denote the total number of nodes, m be the total number of edges, and L be the number of layers. For simplicity, the dimensions of the node hidden features remain constant as d . The complexity of GCN is $O(Lmd + Lnd^2)$, and the complexity of MLP_{GNN}

is $O(Lnd^2)$ [39]. Then we have the complexity of BiKT as $O(tLmd + 3tLnd^2)$.

It should be noted that the computational complexity of the BiKT-enhanced GNN is equivalent to that of the original GNN during inference. If we directly use the derived MLP for inference, the computational complexity will be significantly less than the original GNN.

5 EXPERIMENTAL RESULTS AND ANALYSIS

5.1 Experimental Settings

Datasets and Model Architectures. Seven widely used node classification benchmarks are adopted in our experiments, including three citation networks (Cora, Citeseer, and Pubmed [27], [40]), two product co-occurrence networks (A-computer and A-photo [41]), two heterophilic networks (Chameleon and Squirrel), and two large-scale OGB datasets (OGB-Arxiv and OGB-Products [42]). Meanwhile, to validate the knowledge transfer capability of BiKT under different architectures, several typical GNNs with different architectures are adopted, including GCN [26], GAT [8], FAGCN [14], GCNII [25], and MixHop [9]. Besides, we also adopt two bioinformatics datasets and a large dataset from OGB [42], including MUTAG, PTC, and OGB-molhiv, to verify the effectiveness of BiKT on the graph classification task. GCN and GIN as two classical GNNs for graph classification are employed as backbones.

Experimental Setup. To comprehensively evaluate our method, the dataset is split into training/validation/testing using the **sparse split ratio (2.5%/2.5%/95%)** for semi-supervised node classification. Notably, for the large-scale Arxiv and Products datasets, we follow the same official splitting provided in OGB [42]. For the experiments, we conduct the node classification task in two settings: transductive (*tran*) and inductive (*ind*) setting. Specifically, we follow the setting in [20], for the inductive setting, there are 80% samples of the test set can be seen in the training phase, while the rest do not participate in the training. We report the mean and standard deviation of 10 independent runs performed with different random seeds. Accuracy is used to measure the model performance. For the graph classification task, following the experimental setting in [13], we report the average and standard deviation of validation accuracies across the 10 folds within the cross-validation for the MUTAG and PTC datasets. For the OGB-molhiv dataset, we adopt the official splitting provided in OGB [42] and also report the mean and standard deviation of 10 independent runs.

Baseline Implementation. For FAGCN, GCN, and GAT, we directly use the open-source codes released in [14]. For the others, we re-implement the models that refer to the open source code based on Deep Graph library [43]. For each model, we use hyperopt [44] to search for the optimal hyperparameters. Specifically, the search space for each hyperparameter is: learning rate within $\{0.001, 0.005, 0.01, 0.05\}$, dropout rate with $\{0.1, 0.2, 0.3, 0.4, 0.5, 0.6, 0.7, 0.8, 0.9\}$, weight decay rate within $\{1e-5, 5e-5, 1e-4, 5e-4, 1e-3, 5e-3\}$, hidden units within $\{16, 32, 64, 128, 256\}$.

TABLE 2

Results of the node classification task under the transductive setting, where red letters denote the performance gains brought by BiKT compared to the base MLP_{GNN} and GNN, respectively.

Method	Cora	Citeseer	Pubmed	A-computer	A-photo	Chameleon	Squirrel
MLP _{GNN}	49.84±2.19	53.77±2.13	79.22±0.77	72.69±0.91	79.51±1.67	27.60±2.17	22.83±1.14
BiKT-MLP _{GNN}	74.99±2.54	69.61±1.55	85.15±0.93	81.26±1.74	90.58±1.05	39.69±3.03	31.42±2.39
GNN	73.44±1.96	65.97±2.46	81.62±0.90	83.47±1.34	90.10±0.74	39.22±3.59	30.44±2.09
BiKT-GNN	76.91±2.87	68.63±2.06	82.28±0.46	84.24±1.05	90.90±0.74	41.48±2.53	31.19±1.87
Improv. (MLP/GNN)	25.15/3.47	15.84/2.66	5.93/0.66	8.57/0.77	11.07/0.80	12.09/2.26	8.59/0.75
MLP _{GAT}	47.80±2.41	49.41±1.95	79.61±0.72	69.68±1.09	74.60±1.60	39.83±2.07	22.78±1.58
BiKT-MLP _{GAT}	71.60±3.16	60.79±2.33	82.53±0.72	82.68±1.47	87.51±2.98	41.34±2.89	29.77±1.75
GAT	72.67±3.80	64.43±3.08	81.32±0.71	83.42±1.68	88.14±2.08	41.27±2.58	27.01±1.71
BiKT-GAT	77.40±1.50	67.11±1.70	81.91±0.54	84.48±1.17	90.65±0.54	42.89±3.91	27.69±1.77
Improv. (MLP/GNN)	23.80/4.73	11.38/2.68	2.92/0.59	13.00/1.06	12.91/2.51	1.51/1.62	6.99/0.68
MLP _{FAGCN}	48.77±2.64	52.16±2.82	80.13±0.76	70.14±1.19	78.29±2.28	31.78±6.92	22.96±2.43
BiKT-MLP _{FAGCN}	73.64±2.98	68.21±1.72	82.83±1.14	78.68±1.95	89.31±1.30	39.70±4.42	26.62±2.05
FAGCN	77.23±1.70	67.47±1.71	83.33±0.92	83.19±1.25	91.03±1.20	41.82±3.94	27.09±1.96
BiKT-FAGCN	79.00±1.65	68.79±3.10	84.14±0.61	84.49±0.97	92.16±0.28	43.07±3.43	28.10±1.65
Improv. (MLP/GNN)	24.87±1.77	16.05±1.32	2.70 ±0.81	8.54±1.30	11.02±1.13	7.92±1.25	3.66±1.01
MLP _{GCNII}	49.75±2.69	52.22±2.53	79.95±0.75	71.28±1.10	78.97±1.59	37.19±2.45	25.00±1.80
BiKT-MLP _{GCNII}	75.72±2.72	68.92±2.17	86.05±0.52	84.39±0.91	92.25±1.00	41.69±2.90	30.05±1.33
GCNII	79.45±0.92	68.36±1.63	83.98±1.09	84.82±1.00	90.64±1.73	40.26±2.85	27.85±2.70
BiKT-GCNII	80.19±1.40	69.35±1.81	85.09±0.40	85.40±1.07	91.93±0.75	42.78±3.30	29.11±1.67
Improv. (MLP/GNN)	25.97±0.74	16.70±0.99	6.10±1.11	13.11±0.58	13.28±1.29	4.50±2.52	5.05±1.26
MLP _{MixHop}	48.04±3.93	49.28±2.87	79.48±1.15	71.30±1.31	78.17±2.15	27.46±4.28	21.78±0.84
BiKT-MLP _{MixHop}	77.49±1.15	68.11±1.78	85.55±0.72	82.96±1.15	91.26±1.16	34.93±3.85	29.70±2.32
MixHop	74.60±1.96	62.64±2.26	84.62±0.65	78.98±1.23	87.44±1.58	37.52±7.07	27.55±3.53
BiKT-MixHop	79.43±2.29	68.28±1.55	85.68±0.73	83.58±1.17	91.44±1.40	39.24±5.27	28.91±1.78
Improv. (MLP/GNN)	29.45±4.83	18.83±5.64	6.07±1.06	11.66±4.60	13.09±4.00	7.47±1.72	7.92±1.36

5.2 Performance Comparison

For the node classification task, the performance in the transductive setting of our method on five popular benchmarks is presented in Table 2. It can be observed that, after knowledge transfer between the host GNN and the latent MLP, the BiKT-GNN under the five architectures consistently outperforms the original models on all datasets by a large margin, e.g., exceeding the MixHop by 6.86% on the Citeseer dataset. On the datasets with large-scale, we adopt GraphSAGE as the backbone and present the experimental results under two settings in Table 4. It can be seen that the proposed BiKT can still bring some improvement to the GNN on large-scale graphs. Intriguingly, our BiKT-MLP_{GNN} also achieves significant performance improvements on some datasets, even surpassing BiKT-GNN, e.g., achieving a 2.87% improvement on the Citeseer dataset under the GCN architecture. With the above promising results, it can be concluded that: 1) BiKT could be helpful for GNN to further leverage the capabilities of the T operation to capture information from node content features without modifying the existing architecture of the GNN. 2) With the effective integration of topological information, MLPs could be as good as GNNs. This implies that further study of graph-based MLPs on other graph-related tasks is also a worthwhile research direction.

Meanwhile, we also evaluate the performance comparison of MLPs under the inductive setting to verify would the enhanced MLP via BiKT perform well without the explicit topology guidance. It can be seen from Table 3 that regardless of the GNN architecture, the BiKT-MLP_{GNN} outperforms the MLP by a significant margin in most cases, e.g., obtaining an improvement in the range from **0.60% to 10.30%** on the five datasets under the GCNII architecture. In addition, BiKT-MLP_{GNN} also shows its superiority compared to MLP_{GNN}. The remarkable performance indicates

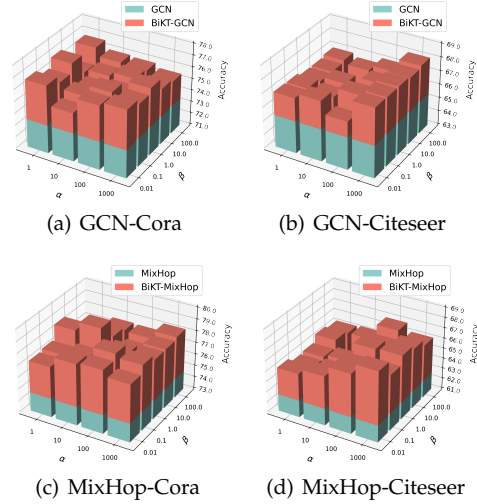


Fig. 6. The effect of different values of α and β on performance gain.

that BiKT can not only effectively transfer the topological knowledge from GNN to MLP_{GNN}, but also improve the ability of MLP_{GNN} to capture knowledge from the node content features, enabling it to perform well even when there is no topological structure.

It can be seen from Table 5 that BiKT also has the ability to enhance the performance of GNNs for the graph classification task. More concretely, GCN and GAT also achieved performance gains of 1.90% and 0.38% on OGB-molhiv, respectively. It indicates that the graph classification task can also benefit by strengthening the feature transformation operations of GNNs except for strengthening the feature propagation operations.

TABLE 3

Results of the node classification task under the inductive setting, where red letters denote the performance gains brought by BiKT compared to the base MLP_{GNN} and GNN, respectively.

Method	Cora	Citeseer	Pubmed	A-computer	A-photo	Chameleon	Squirrel
MLP _{GNN}	54.47±3.31	58.54±2.43	76.47±3.44	58.21±6.51	79.42±2.69	26.31±2.00	24.27±1.63
BiKT-MLP _{GNN}	65.70±3.14	65.52±3.97	84.19±1.13	79.54±0.94	87.15±1.01	38.72±3.21	30.14±2.74
GCN	75.18±1.73	65.32±2.01	83.71±1.30	84.26±1.55	91.11±0.69	38.97±3.12	30.09±2.62
BiKT-GCN	76.60±1.72	67.20±2.41	84.19±0.45	85.92±1.26	92.03±0.76	40.12±2.25	30.55±2.52
Improv. (MLP/GNN)	11.23/1.42	6.98/1.88	7.72/0.48	21.33/1.66	7.73/0.92	12.41/1.15	5.87/0.46
MLP _{GAT}	49.75±5.93	51.33±4.54	79.53±1.09	57.39±12.4	64.82±12.5	39.34±2.46	23.09±1.16
BiKT-MLP _{GAT}	62.20±3.47	59.29±2.07	82.33±0.63	79.37±2.47	84.76±1.66	40.55±3.20	29.28±1.36
GAT	72.55±2.80	63.14±2.32	81.46±0.81	80.50±1.31	84.14±1.60	40.06±3.07	27.73±1.13
BiKT-GAT	75.40±0.66	66.39±1.21	81.81±0.66	83.23±2.03	89.62±1.54	42.16±3.46	27.89±1.34
Improv. (MLP/GNN)	12.45/2.85	7.96/3.25	2.80/0.35	21.98/2.73	19.94/5.48	1.21/2.10	6.19/0.16
MLP _{FAGCN}	60.72±1.84	58.84±2.46	80.47±0.61	69.16±2.44	77.42±2.56	31.25±6.39	23.45±2.26
BiKT-MLP _{FAGCN}	67.10±3.00	65.49±2.13	82.72±0.49	77.57±1.31	88.12±1.50	40.28±4.60	26.26±2.49
FAGCN	73.19±3.58	68.21±3.00	82.49±1.92	84.20±0.85	92.13±2.10	41.57±4.25	27.70±1.81
BiKT-FAGCN	76.00±2.17	69.76±2.26	84.10±1.55	85.07±1.15	92.47±2.31	42.57±3.08	28.75±1.09
Improv. (MLP/GNN)	6.38/2.81	6.65/1.55	2.25/1.61	8.41/0.87	10.70/0.34	9.03/1.00	2.81/1.05
MLP _{GCNII}	62.41±2.24	60.36±2.82	78.91±1.34	69.16±2.44	80.69±2.11	36.62±2.61	25.47±1.26
BiKT-MLP _{GCNII}	66.91±3.38	63.69±3.51	84.92±0.62	83.51±0.81	88.71±2.25	40.92±2.35	30.56±0.76
GCNII	80.01±0.31	67.39±1.19	84.98±0.76	83.41±1.25	91.94±0.77	39.12±2.45	27.40±3.38
BiKT-GCNII	81.02±0.90	68.22±1.60	85.66±0.89	84.53±2.15	92.90±0.37	41.84±2.67	29.41±2.37
Improv. (MLP/GNN)	4.50/1.01	3.33/0.83	6.01/0.68	14.35/1.12	8.02/0.96	4.30/2.72	5.09/2.01
MLP _{MixHop}	59.81±3.61	55.60±3.88	79.38±1.00	59.56±9.23	72.27±5.12	26.81±3.47	22.37±1.24
BiKT-MLP _{MixHop}	65.47±3.81	65.24±3.52	84.22±0.53	78.55±1.74	87.45±1.74	31.56±4.33	29.34±2.04
MixHop	71.27±1.87	63.11±2.16	82.42±0.27	82.90±1.64	89.55±1.50	36.05±7.77	27.80±3.32
BiKT-MixHop	75.43±1.20	66.28±1.69	84.68±1.34	85.58±1.26	90.44±0.93	38.18±4.81	28.49±1.45
Improv. (MLP/GNN)	5.66/4.16	9.64/3.17	4.84/2.26	18.99/2.68	15.18/0.89	4.75/2.13	6.97/0.69

TABLE 4

Results of the node classification task on the large-scale datasets.

Datasets	Eval	SAGE	BiKT-SAGE	Improv.
OGB-Arxiv	<i>transductive</i>	74.55±0.69	75.47±0.21	↑ 0.92
	<i>inductive</i>	71.37±0.71	71.71±0.46	↑ 0.34
OGB-Products	<i>transductive</i>	78.98±0.14	79.69±0.27	↑ 0.71
	<i>inductive</i>	76.98±0.41	77.47±0.41	↑ 0.49

TABLE 5

Results of the graph classification task on three datasets.

Method	MUTAG	PTC	OGB-molhiv
GCN	84.16 ± 6.40	61.86 ± 5.21	75.25 ± 2.07
BiKT-GCN	87.26 ± 5.01	65.00 ± 4.67	77.15 ± 1.22
Improve.	3.10	3.14	1.90
GIN	87.22 ± 7.45	62.31 ± 6.29	76.09 ± 1.43
BiKT-GIN	90.13 ± 7.28	65.47 ± 5.99	76.47 ± 1.81
Improve.	2.91	3.16	0.38

5.3 Sensitivity Analysis of BiKT

Hyperparameter Analysis. We analyze the impact of the coefficients α and β on model performance using GCN and MixHop architectures. As shown in Fig. 6, the BiKT-GCN holds a clear performance improvement over the original model, regardless of the parameter settings. The inspiring results show that the generalization ability of our BiKT-GCN is not heavily reliant on hyperparameter tuning. More concretely, both GCN and Mixhop behave relatively sensitive to α on the Citeseer dataset, and the larger the α is, the greater the performance gain. While the two GNNs seem to be more impacted by β on the Cora dataset.

Analysis of the Recurrent Training. We report the performance gains when performing the number of iterations from 0 to 7 to verify the role of the recurrent training strategy for

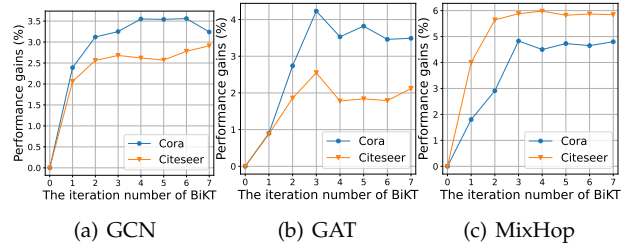


Fig. 7. The performance gains when performing the number of iterations in the recurrent training from 0 to 7.

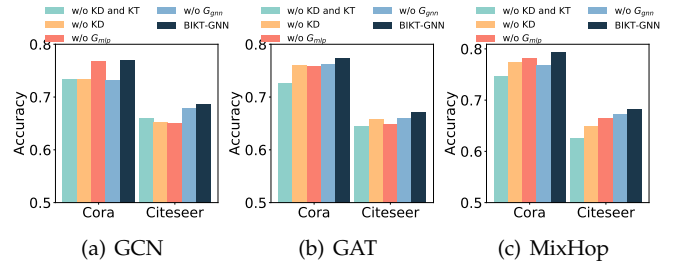


Fig. 8. Effectiveness evaluation of knowledge transfer (KT) and knowledge distillation (KD), where knowledge transfer denotes specifically the process of representation generation via generators G_{gnn} and G_{mlp} .

BiKT. We can see from Fig. 7 that the performance gains of GCN, GAT, and MixHop on both datasets stabilize as the number of iterations increases. As past a certain extent of knowledge transference, the latent potential of the feature transformation operations will be thoroughly harnessed, thus stabilizing the performance.

TABLE 6
The MMD distances between the representation distribution of generators and models at different training epochs.

	Dataset	Initial	50-th Epoch	100-th Epoch
MMD(GCN, G_{gnn})	Cora	4.521	1.531	0.746
	Citeseer	5.079	1.262	0.530
MMD(MLP, G_{mlp})	Cora	4.435	0.642	-
	Citeseer	4.615	1.527	0.532
MMD(GAT, G_{gnn})	Cora	4.623	1.270	0.638
	Citeseer	6.339	1.262	-
MMD(MLP, G_{mlp})	Cora	4.800	2.513	0.955
	Citeseer	5.127	0.960	-

5.4 Ablation Study

Effectiveness of knowledge extraction. To analyze the contributions of knowledge transfer (KT) and knowledge distillation (KD) in Eq. (7), an ablation study of BiKT is conducted on Cora and Citeseer datasets. As shown in Fig. 8, each term of Eq. (7) has a positive effect on GNN. Interestingly, for GCN as the base GNN, either part alone has a general gain on two datasets, but a more significant gain is achieved when both are used together. It can also be observed that, the impact of G_{gnn} is stable and moderate, regardless of the GNN used. On the contrary, the impact of G_{mlp} varies widely with architecture and dataset.

Effectiveness of parameter inheritance. To illustrate the necessity of sharing parameters between the GNN and MLP_{GNN} , we perform a comparison of GNN with re-initialized MLP (denoted as BiKT-GNN w/ MLP^{re}) in the BiKT framework. As shown in Fig. 9, the performance gains brought by BiKT-GNN w/ MLP^{re} are modest compared to BiKT-GNN. Besides, it may instead degrade the model’s performance in some cases. The experimental results illustrate that the parameter inheritance scheme has a more stable performance, in comparison to re-initialization.

5.5 Analysis of Generators for Distribution Modeling

To quantitatively analyze whether the generator is capable of efficiently modeling the representation distribution of the model with Eq. (4), we calculate the MMD distances between the representation generated by generators at different training epochs and the representation output by the model. The results are reported in Table 6. It can be observed that as the training of the generator progresses, the distribution of its generated representations gradually becomes closer to the target representation distribution. This indicates the effectiveness of the optimization objective set for the generator and aligns with our expectations.

6 DISCUSSION

Recently, a lot of efforts have been made in data augmentation over graphs [45], [46], [47]. In general, existing data augmentation methods start from the topological structure of the graph and propose a series of methods to perturb the connectivity of the graph [45], [48], [49]. Differently, our BiKT conducts the augmentation from the representation space without modifying the topological structure and node features. BiKT is therefore orthogonal to these methods and can be used simultaneously. Particularly, similar ideas have

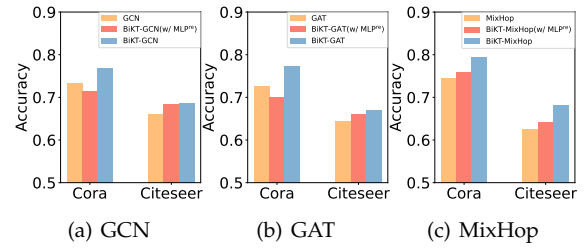


Fig. 9. The effectiveness evaluation of parameter inheritance stagy.

also been applied to other fields, such as image translation [50] and federal learning [51].

In addition, several works have also emerged in recent years aimed at exploring the connection between GNNs and MLPs [52], [53] and how MLPs can be used as an alternative to GNNs on graph-related tasks [20], [54], [55]. To this end, these approaches introduce techniques such as regularization [56] and data augmentation [21] to improve the performance of MLP on graph data. In contrast, the objective of this paper is to discover a method to enhance GNNs through feature transformation and MLP_{GNN} . We also propose to examine the relationship between GNNs and MLPs through the perspective of domain adaptation. Notably, the approach presented in [53] can be viewed as a specific instance of BiKT.

7 CONCLUSION

In this work, we point out the existing GNNs have not effectively unleashed the potential of feature transformation operations therein with the empirical investigation. To address this issue, we propose a generic framework, BiKT, to capture the induced distribution from the GNN and the derived model composed by feature transformation operations, thus improving them together. Moreover, we introduce a new perspective from domain adaption to unpack the connection between GNNs and MLPs, and provide a theoretical analysis of our approach. Extensive experiments on 7 datasets with 6 GNNs as backbones demonstrate that BiKT is not only highly conducive for GNN to further leverage the capabilities of the T operation, but also greatly boost the performance of latent MLP derived from the GNN.

REFERENCES

- [1] F. Xia, K. Sun, S. Yu, A. Aziz, L. Wan, S. Pan, and H. Liu, “Graph learning: A survey,” *IEEE Transactions on Artificial Intelligence*, vol. 2, no. 2, pp. 109–127, 2021.
- [2] X. He, K. Deng, X. Wang, Y. Li *et al.*, “Lightgcn: Simplifying and powering graph convolution network for recommendation,” in *Proc. 43rd Int. ACM SIGIR Conf. on Res. Dev. in Inf. Retr.*, 2020, pp. 639–648.
- [3] X. Wang, X. He, M. Wang, F. Feng, and T.-S. Chua, “Neural graph collaborative filtering,” in *Proc. 42nd Int. ACM SIGIR Conf. on Res. Dev. in Inf. Retr.*, 2019, pp. 165–174.
- [4] M. Qu, H. Cai, and J. Tang, “Neural structured prediction for inductive node classification,” *arXiv preprint arXiv:2204.07524*, 2022.
- [5] K. Yan, Y. Liu, Y. Lin, and S. Ji, “Periodic graph transformers for crystal material property prediction,” *arXiv preprint arXiv:2209.11807*, 2022.
- [6] S. Zheng, Z. Zhu, Z. Liu *et al.*, “Multi-modal graph learning for disease prediction,” *IEEE Trans. Medical Imaging*, 2022.

- [7] M. Zitnik, M. Agrawal, and J. Leskovec, "Modeling polypharmacy side effects with graph convolutional networks," *Bioinformatics*, vol. 34, no. 13, pp. i457–i466, 2018.
- [8] P. Veličković, G. Cucurull, A. Casanova *et al.*, "Graph attention networks," in *Proc. Int. Conf. Learn. Represent.*, 2018.
- [9] S. Abu-El-Haija, B. Perozzi, A. Kapoor, N. Alipourfard *et al.*, "Mix-hop: Higher-order graph convolutional architectures via sparsified neighborhood mixing," in *Proc. 36th Int. Conf. on Mach. Learn.* PMLR, 2019, pp. 21–29.
- [10] F. Frasca, E. Rossi, D. Eynard, B. Chamberlain, M. Bronstein, and F. Monti, "Sign: Scalable inception graph neural networks," *arXiv preprint arXiv:2004.11198*, 2020.
- [11] J. Klicpera, A. Bojchevski, and S. Günnemann, "Predict then propagate: Graph neural networks meet personalized pagerank," *arXiv preprint arXiv:1810.05997*, 2018.
- [12] F. Wu, A. Souza, T. Zhang *et al.*, "Simplifying graph convolutional networks," in *Proc. 36th Int. Conf. on Mach. Learn.* PMLR, 2019, pp. 6861–6871.
- [13] K. Xu, W. Hu, J. Leskovec, and S. Jegelka, "How powerful are graph neural networks?" *arXiv preprint arXiv:1810.00826*, 2018.
- [14] D. Bo, X. Wang, C. Shi, and H. Shen, "Beyond low-frequency information in graph convolutional networks," in *Proc. 35th AAAI Conf. Artif. Intell.*, vol. 35, no. 5, 2021, pp. 3950–3957.
- [15] B. Chamberlain, J. Rowbottom, M. I. Gorinova, M. Bronstein, S. Webb, and E. Rossi, "Grand: Graph neural diffusion," in *Proc. 38th Int. Conf. on Mach. Learn.* PMLR, 2021, pp. 1407–1418.
- [16] K. Kong, G. Li, M. Ding, Z. Wu, C. Zhu, B. Ghanem, G. Taylor, and T. Goldstein, "Robust optimization as data augmentation for large-scale graphs," in *Proceedings of the IEEE/CVF Conference on Computer Vision and Pattern Recognition*, 2022, pp. 60–69.
- [17] Y. You, T. Chen, Y. Sui, T. Chen, Z. Wang, and Y. Shen, "Graph contrastive learning with augmentations," *Advances in neural information processing systems*, vol. 33, pp. 5812–5823, 2020.
- [18] Q. Li, Z. Han, and X.-M. Wu, "Deeper insights into graph convolutional networks for semi-supervised learning," in *Proceedings of the AAAI conference on artificial intelligence*, vol. 32, no. 1, 2018.
- [19] K. Sun, Z. Lin, and Z. Zhu, "Multi-stage self-supervised learning for graph convolutional networks on graphs with few labeled nodes," in *Proceedings of the AAAI conference on artificial intelligence*, vol. 34, no. 04, 2020, pp. 5892–5899.
- [20] S. Zhang, Y. Liu, Y. Sun, and N. Shah, "Graph-less neural networks: Teaching old mlps new tricks via distillation," *The 10th Int. Conf. on Learn. Represent.*, 2022.
- [21] L. Wu, J. Xia, H. Lin, Z. Gao, Z. Liu, G. Zhao, and S. Z. Li, "Teaching yourself: c graph self-distillation on neighborhood for node classification," *arXiv preprint arXiv:2210.02097*, 2022.
- [22] Y. Tian, C. Zhang, Z. Guo, X. Zhang, and N. Chawla, "Learning mlps on graphs: A unified view of effectiveness, robustness, and efficiency," in *The 11th Int. Conf. on Learn. Represent.*, 2023.
- [23] W. Zheng, E. W. Huang, N. Rao, S. Kataria, Z. Wang, and K. Subbian, "Cold brew: Distilling graph node representations with incomplete or missing neighborhoods," in *The 10th Int. Conf. on Learn. Represent.*, 2022.
- [24] W. Hamilton, Z. Ying, and J. Leskovec, "Inductive representation learning on large graphs," in *Proc. Adv. Neural Inf. Process. Syst.*, 2017, pp. 1024–1034.
- [25] M. Chen, Z. Wei, Z. Huang, B. Ding, and Y. Li, "Simple and deep graph convolutional networks," in *Proc. 37th Int. Conf. on Mach. Learn.* PMLR, 2020, pp. 1725–1735.
- [26] T. N. Kipf and M. Welling, "Semi-supervised classification with graph convolutional networks," *arXiv preprint arXiv:1609.02907*, 2016.
- [27] P. Sen, G. Namata *et al.*, "Collective classification in network data," *AI magazine*, vol. 29, no. 3, pp. 93–93, 2008.
- [28] J. Zhu, Y. Yan, L. Zhao, M. Heimann, L. Akoglu, and D. Koutra, "Beyond homophily in graph neural networks: Current limitations and effective designs," *Proc. Adv. Neural Inf. Process. Syst. (NerulPS)*, vol. 33, pp. 7793–7804, 2020.
- [29] P. W. Battaglia, J. B. Hamrick, V. Bapst, A. Sanchez-Gonzalez *et al.*, "Relational inductive biases, deep learning, and graph networks," *arXiv preprint arXiv:1806.01261*, 2018.
- [30] G. Hinton, O. Vinyals, and J. Dean, "Distilling the knowledge in a neural network," *arXiv preprint arXiv:1503.02531*, 2015.
- [31] D. P. Kingma and M. Welling, "Auto-encoding variational bayes," *arXiv preprint arXiv:1312.6114*, 2013.
- [32] I. Goodfellow, J. Pouget-Abadie, M. Mirza, B. Xu, D. Warde-Farley, S. Ozair, A. Courville, and Y. Bengio, "Generative adversarial networks," *Communications of the ACM*, vol. 63, no. 11, pp. 139–144, 2020.
- [33] R. Rombach, A. Blattmann, D. Lorenz, P. Esser, and B. Ommer, "High-resolution image synthesis with latent diffusion models," in *Proceedings of the IEEE/CVF Conference on Computer Vision and Pattern Recognition*, 2022, pp. 10684–10695.
- [34] Q. Mao, H.-Y. Lee, H.-Y. Tseng, S. Ma, and M.-H. Yang, "Mode seeking generative adversarial networks for diverse image synthesis," in *Proceedings of the IEEE/CVF conference on computer vision and pattern recognition*, 2019, pp. 1429–1437.
- [35] L. Wang, X. Zhang, H. Su, and J. Zhu, "A comprehensive survey of continual learning: Theory, method and application," *arXiv preprint arXiv:2302.00487*, 2023.
- [36] A. Blum and T. Mitchell, "Combining labeled and unlabeled data with co-training," in *Proceedings of the eleventh annual conference on Computational learning theory*, 1998, pp. 92–100.
- [37] S. Ben-David, J. Blitzer, K. Crammer, and F. Pereira, "Analysis of representations for domain adaptation," *Advances in neural information processing systems*, vol. 19, 2006.
- [38] J. Blitzer, K. Crammer, A. Kulesza, F. Pereira, and J. Wortman, "Learning bounds for domain adaptation," *Advances in neural information processing systems*, vol. 20, 2007.
- [39] Z. Wu, S. Pan, F. Chen *et al.*, "A comprehensive survey on graph neural networks," *IEEE transactions on neural networks and learning systems*, vol. 32, no. 1, pp. 4–24, 2020.
- [40] Z. Yang, W. Cohen, and R. Salakhudinov, "Revisiting semi-supervised learning with graph embeddings," in *International conference on machine learning*. PMLR, 2016, pp. 40–48.
- [41] O. Shchur, M. Mumme, A. Bojchevski, and S. Günnemann, "Pitfalls of graph neural network evaluation," *arXiv preprint arXiv:1811.05868*, 2018.
- [42] W. Hu, M. Fey, M. Zitnik, Y. Dong, H. Ren, B. Liu, M. Catasta, and J. Leskovec, "Open graph benchmark: Datasets for machine learning on graphs," *Advances in neural information processing systems*, vol. 33, pp. 22118–22133, 2020.
- [43] M. Wang, D. Zheng, Z. Ye, Q. Gan, M. Li, X. Song, J. Zhou, C. Ma, L. Yu, Y. Gai *et al.*, "Deep graph library: A graph-centric, highly-performant package for graph neural networks," *arXiv preprint arXiv:1909.01315*, 2019.
- [44] J. Bergstra, D. Yamins, and D. Cox, "Making a science of model search: Hyperparameter optimization in hundreds of dimensions for vision architectures," in *Proc. 30th Int. Conf. on Mach. Learn.*, 2013, pp. 115–123.
- [45] T. Zhao, Y. Liu, L. Neves, O. Woodford, M. Jiang, and N. Shah, "Data augmentation for graph neural networks," in *Proceedings of the aai conference on artificial intelligence*, vol. 35, no. 12, 2021, pp. 11015–11023.
- [46] W. Feng, J. Zhang, Y. Dong, Y. Han, H. Luan, Q. Xu, Q. Yang, E. Kharlamov, and J. Tang, "Graph random neural networks for semi-supervised learning on graphs," *Advances in neural information processing systems*, vol. 33, pp. 22092–22103, 2020.
- [47] V. Verma, M. Qu, K. Kawaguchi, A. Lamb, Y. Bengio, J. Kannala, and J. Tang, "Graphmix: Improved training of gnns for semi-supervised learning," in *Proceedings of the AAAI conference on artificial intelligence*, vol. 35, no. 11, 2021, pp. 10024–10032.
- [48] Y. Rong, W. Huang, T. Xu, and J. Huang, "Dropege: Towards deep graph convolutional networks on node classification," *arXiv preprint arXiv:1907.10903*, 2019.
- [49] D. Chen, Y. Lin, W. Li, P. Li, J. Zhou, and X. Sun, "Measuring and relieving the over-smoothing problem for graph neural networks from the topological view," in *Proceedings of the AAAI conference on artificial intelligence*, vol. 34, no. 04, 2020, pp. 3438–3445.
- [50] J. Hoffman, E. Tzeng, T. Park, J.-Y. Zhu, P. Isola, K. Saenko, A. Efros, and T. Darrell, "Cycada: Cycle-consistent adversarial domain adaptation," in *International conference on machine learning*. Pmlr, 2018, pp. 1989–1998.
- [51] Z. Zhu, J. Hong, and J. Zhou, "Data-free knowledge distillation for heterogeneous federated learning," in *International Conference on Machine Learning*. PMLR, 2021, pp. 12878–12889.
- [52] C. Yang, Q. Wu, J. Wang, and J. Yan, "Graph neural networks are inherently good generalizers: Insights by bridging gnns and mlps," *arXiv preprint arXiv:2212.09034*, 2022.
- [53] X. Han, T. Zhao, Y. Liu, X. Hu, and N. Shah, "MLPinit: Embarrassingly simple GNN training acceleration with MLP initialization," in *International Conference on Learning Representations*, 2023.
- [54] W. Zhang, Z. Yin, Z. Sheng, Y. Li, W. Ouyang, X. Li, Y. Tao, Z. Yang, and B. Cui, "Graph attention multi-layer perceptron,"

in *Proceedings of the 28th ACM SIGKDD Conference on Knowledge Discovery and Data Mining*, 2022, pp. 4560–4570.

- [55] L. Chen, Z. Chen, and J. Bruna, “On graph neural networks versus graph-augmented mlps,” *arXiv preprint arXiv:2010.15116*, 2020.
 [56] Y. Hu, H. You, Z. Wang, Z. Wang, E. Zhou, and Y. Gao, “Graph-mlp: Node classification without message passing in graph,” *arXiv preprint arXiv:2106.04051*, 2021.

APPENDIX

Derivations of Proposition 4.1

Proposition 4.1. *Let $q(\mathbf{z}|y)$ be the distribution modeled by generator G , $p(y|\mathbf{z}; f_{cls})$ and $p(\mathbf{z}|y; f_{cls})$ be the posterior distribution and the corresponding induce distribution of f_{cls} . Then maximizing $H(q(\mathbf{z}|y)) + \mathbb{E}_{y \sim p(y)} \mathbb{E}_{\mathbf{z} \sim q(\mathbf{z}|y)} [\log p(y|\mathbf{z})]$ is equivalent to minimizing the conditional KL-divergence between $q(\mathbf{z}|y)$ and $p(\mathbf{z}|y; f_{cls})$, i.e., $D_{KL}[q(\mathbf{z}|y) \| p(\mathbf{z}|y; f_{cls})]$.*

Proof. According to the definition of D_{KL} , $D_{KL}(q(\mathbf{z}|y) \| p(\mathbf{z}|y; f_{cls}))$ can be expanded as:

$$\begin{aligned} & D_{KL}[q(\mathbf{z}|y) \| p(\mathbf{z}|y; f_{cls})] \\ &= \mathbb{E}_{y \sim p(y)} \left[\mathbb{E}_{\mathbf{z} \sim q(\mathbf{z}|y)} \left[\log \frac{q(\mathbf{z}|y)}{p(\mathbf{z}|y; f_{cls})} \right] \right] \\ &= \mathbb{E}_{y \sim p(y)} \mathbb{E}_{\mathbf{z} \sim q(\mathbf{z}|y)} [\log q(\mathbf{z}|y)] \\ &\quad - \mathbb{E}_{y \sim p(y)} \mathbb{E}_{\mathbf{z} \sim q(\mathbf{z}|y)} [\log p(\mathbf{z}|y; f_{cls})] \\ &= -H(q(\mathbf{z}|y)) - \mathbb{E}_{y \sim p(y)} \mathbb{E}_{\mathbf{z} \sim q(\mathbf{z}|y)} [\log p(\mathbf{z}|y; f_{cls})] \end{aligned} \quad (9)$$

For the second term, it can be rewritten based on the Bayes Rule:

$$\begin{aligned} & \mathbb{E}_{y \sim p(y)} \mathbb{E}_{\mathbf{z} \sim q(\mathbf{z}|y)} [\log p(\mathbf{z}|y; f_{cls})] \\ &= \mathbb{E}_{\mathbf{z} \sim q(\mathbf{z}|y)} \left[\log \frac{p(y|\mathbf{z}; f_{cls})p(\mathbf{z})}{p(y)} \right] \\ &= \mathbb{E}_{y \sim p(y)} \mathbb{E}_{\mathbf{z} \sim q(\mathbf{z}|y)} [\log p(y|\mathbf{z}; f_{cls}) + \log p(\mathbf{z}) - \log p(y)] \end{aligned} \quad (10)$$

Since $\log p(\mathbf{z})$ and $\log p(y)$ are the prior distribution that is constant w.r.t $q(\mathbf{z}|y)$, therefore, we can obtain the follows by substituting Eq. (10) into Eq. (9):

$$\begin{aligned} & \arg \min_{q(\mathbf{z}|y)} D_{KL}[q(\mathbf{z}|y) \| p(\mathbf{z}|y; f_{cls})] \\ &\equiv \arg \min_{q(\mathbf{z}|y)} -H(q(\mathbf{z}|y)) \\ &\quad - \mathbb{E}_{y \sim p(y)} \mathbb{E}_{\mathbf{z} \sim q(\mathbf{z}|y)} [\log p(y|\mathbf{z}; f_{cls}) + \log p(\mathbf{z}) - \log p(y)] \\ &\equiv \arg \min_{q(\mathbf{z}|y)} -H(q(\mathbf{z}|y)) - \mathbb{E}_{y \sim p(y)} \mathbb{E}_{\mathbf{z} \sim q(\mathbf{z}|y)} [\log p(y|\mathbf{z}; f_{cls})] \\ &\equiv \arg \max_{q(\mathbf{z}|y)} H(q(\mathbf{z}|y)) + \mathbb{E}_{y \sim p(y)} \mathbb{E}_{\mathbf{z} \sim q(\mathbf{z}|y)} [\log p(y|\mathbf{z}; f_{cls})] \end{aligned} \quad (11)$$

This completes the proof. \square

Derivations of Proposition 4.2

Let’s first introduce some symbols and their definitions from [37] as below:

Assumption 4.1. *Given f_{cls}^{tgt} and f_{cls}^{src} of the target and source models respectively, $q(\mathbf{z}|y)$ can approximate $p(\mathbf{z}|y; f_{cls}^{tag})$ and have $d_{\mathcal{H}}(q(\mathbf{z}|y), p(\mathbf{z}|y; f_{cls}^{tag})) \leq d_{\mathcal{H}}(p(\mathbf{z}|y; f_{cls}^{src}), p(\mathbf{z}|y; f_{cls}^{tag}))$, where $d_{\mathcal{H}}$ denotes the \mathcal{H} -divergence.*

Proposition 4.2. *Suppose assumption 1 holds. Let \mathcal{T} and \mathcal{S} be the source domain and target domain with the distribution \mathcal{D}_s and \mathcal{D}_t , respectively. Let \mathcal{R} be a representation function from \mathcal{X} to \mathcal{Z} .*

Symbols	Definitions
\mathcal{X}	the raw feature space
\mathcal{Z}	the representation space
\mathcal{Y}	the set of class labels
\mathcal{H}	a set of hypothesis h
\mathcal{D}_G	an auxiliary distribution derived from the generator G
B	a probability event
\mathcal{R}	a fixed representation function from \mathcal{X} to \mathcal{Z}
$d_{\mathcal{H}}(\mathcal{D}_1, \mathcal{D}_2)$	the \mathcal{H} -divergence between \mathcal{D}_1 and \mathcal{D}_2
$\epsilon_*(h)$	the expected risk of h on the domain $*$
$\lambda = \min_{h \in \mathcal{H}} (\epsilon_{\mathcal{T}}(h) + \epsilon_{\mathcal{S}}(h))$	the optimal risk on \mathcal{T} and \mathcal{S}

Denote \mathcal{D}_G be an auxiliary distribution derived from a generator G and $\mathcal{D}'_s = \tau \mathcal{D}_G + (1 - \tau) \mathcal{D}_s$. Denote \mathcal{H} be a set of hypothesis with VC-dimension d . Given an empirical dataset $\tilde{\mathcal{D}}_s$ and an augmented dataset $\tilde{\mathcal{D}}'_s$ with $|\tilde{\mathcal{D}}_s| = m$ and $|\tilde{\mathcal{D}}'_s| = m' > m$. Let $J(m, d) = \sqrt{\frac{4}{m} (d \log \frac{2em}{d} + \log \frac{4}{\delta})}$, where e is the base of the natural logarithm. If $(\epsilon_{\mathcal{S}}(h) - \epsilon_{\mathcal{S}'}(h))$ is bounded and $m > \frac{1}{2}d$, then with probability at least $1 - \delta$, for every hypothesis $h \in \mathcal{H}$:

$$\begin{aligned} \epsilon_{\mathcal{T}}(h) &\leq \hat{\epsilon}_{\mathcal{S}'}(h) + J(m', d) + d_{\mathcal{H}}(\tilde{\mathcal{D}}'_s, \tilde{\mathcal{D}}_t) + \lambda' \\ &\leq \hat{\epsilon}_{\mathcal{S}}(h) + J(m, d) + d_{\mathcal{H}}(\tilde{\mathcal{D}}_s, \tilde{\mathcal{D}}_t) + \lambda \end{aligned} \quad (12)$$

where $\epsilon_*(h)$ and $\hat{\epsilon}_*(h)$ are the expected and empirical risk of h on the domain respectively. \mathcal{S}' denotes the augmented source domain with $\tilde{\mathcal{D}}'_s$, $\lambda = \min_h (\epsilon_{\mathcal{T}}(h) + \epsilon_{\mathcal{S}}(h))$ and $\lambda' = \min_h (\epsilon_{\mathcal{T}}(h) + \epsilon_{\mathcal{S}'}(h))$ is the optimal risk on two domains.

Proof. For the proof of Proposition 4.2, we first introduce Lemma A.1 from [37], [38] to give the upper bound for the generalization performance of domain adaption (DA):

Lemma A.1. Generalization Bounds for DA [37]:

Let \mathcal{H} be a hypothesis space of VC-dimension d . Let \mathcal{T}_S and \mathcal{T}_T be the source and target domains, whose data distributions are \mathcal{D}_s and \mathcal{D}_t , and $\tilde{\mathcal{D}}_s, \tilde{\mathcal{D}}_t$ be the induced images of \mathcal{D}_s and \mathcal{D}_t over \mathcal{R} , respectively, s.t., $\mathbb{E}_{z \sim \tilde{\mathcal{D}}_} [B(z)] = \mathbb{E}_{x \sim \mathcal{D}_*} [B(\mathcal{R}(x))]$ when given a probability event B , and so for $\tilde{\mathcal{D}}$. Given an observable dataset with m samples, then with probability at least $1 - \delta$, $\forall h \in \mathcal{H}$:*

$$\begin{aligned} \epsilon_{\mathcal{T}}(h) &\leq \hat{\epsilon}_{\mathcal{S}}(h) + \sqrt{\frac{4}{m} \left(d \log \frac{2em}{d} + \log \frac{4}{\delta} \right)} \\ &\quad + d_{\mathcal{H}}(\tilde{\mathcal{D}}_s, \tilde{\mathcal{D}}_t) + \lambda, \end{aligned} \quad (13)$$

where e is the base of the natural logarithm.

Through substituting \mathcal{D}'_s and $\tilde{\mathcal{D}}'_s$ into Eq. (13), it is not hard to obtain:

$$\epsilon_{\mathcal{T}}(h) \leq \hat{\epsilon}_{\mathcal{S}'}(h) + J(m', d) + d_{\mathcal{H}}(\tilde{\mathcal{D}}'_s, \tilde{\mathcal{D}}_t) + \lambda' \quad (14)$$

The theorem will be proved if we can show that $J(m', d) < j(m, d)$ and $d_{\mathcal{H}}(\tilde{\mathcal{D}}'_s, \tilde{\mathcal{D}}_t) < d_{\mathcal{H}}(\tilde{\mathcal{D}}_s, \tilde{\mathcal{D}}_t)$ when assumption 1 holds with $(\epsilon_{\mathcal{S}}(h) - \epsilon_{\mathcal{S}'}(h)) > 0$ is bounded and $m > \frac{1}{2}d$.

For $J^2(m, d) = \frac{4}{m} (d \log \frac{2em}{d} + \log \frac{4}{\delta})$, it can be divided into two terms $\frac{4}{m} d \log \frac{2em}{d}$ and $\frac{4}{m} \log \frac{4}{\delta}$. For the first term, let $x = \frac{m}{d}$, we have $\frac{4}{m} d \log \frac{2em}{d} = \frac{4}{x} \log 2ex$. We can obtain the derivative of $\frac{4}{x} \log 2ex$ with respect to x as:

$$\frac{d(\frac{4}{x} \log 2ex)}{dx} = -4x^{-2} \log 2x \quad (15)$$

From Eq. (15) we can see that $\frac{4}{x} \log 2ex$ is monotonically decreasing when $x > \frac{1}{2}$. Meanwhile, it is easy to find for the second term that $\frac{4}{m} \log \frac{4}{\delta}$ is also monotonically decreasing when $m > 0$. From the above we can find that $J(m', d) < J(m, d)$ if $m > \frac{1}{2}d$. Moreover, according to the definition of $d_{\mathcal{H}}(\cdot, \cdot)$, it can be derived for $d_{\mathcal{H}}(\tilde{\mathcal{D}}'_s, \tilde{\mathcal{D}}_t)$ that:

$$\begin{aligned}
 & d_{\mathcal{H}}(\tilde{\mathcal{D}}'_s, \tilde{\mathcal{D}}_t) \\
 &= 2 \sup_{\mathcal{A} \in \mathcal{A}_{\mathcal{H}}} \left| \mathbb{E}_{\mathbf{z} \sim \tilde{\mathcal{D}}'_s} [\Pr(\mathcal{A}(\mathbf{z}))] - \mathbb{E}_{\mathbf{z} \sim \tilde{\mathcal{D}}_t} [\Pr(\mathcal{A}(\mathbf{z}))] \right| \\
 &= 2 \sup_{\mathcal{A} \in \mathcal{A}_{\mathcal{H}}} \left| \tau \mathbb{E}_{\mathbf{z} \sim \tilde{\mathcal{D}}_s} [\Pr(\mathcal{A}(\mathbf{z}))] - \tau \mathbb{E}_{\mathbf{z} \sim \tilde{\mathcal{D}}_t} [\Pr(\mathcal{A}(\mathbf{z}))] \right. \\
 &\quad \left. + (1 - \tau) \mathbb{E}_{\mathbf{z} \sim \tilde{\mathcal{D}}_G} [\Pr(\mathcal{A}(\mathbf{z}))] - (1 - \tau) \mathbb{E}_{\mathbf{z} \sim \tilde{\mathcal{D}}_t} [\Pr(\mathcal{A}(\mathbf{z}))] \right| \\
 &\leq \tau d_{\mathcal{H}}(\tilde{\mathcal{D}}_s, \tilde{\mathcal{D}}_t) + (1 - \tau) d_{\mathcal{H}}(\tilde{\mathcal{D}}_G, \tilde{\mathcal{D}}_t)
 \end{aligned} \tag{16}$$

According to Assumption 1 that $d_{\mathcal{H}}(q(\mathbf{z}|y), p(\mathbf{z}|y; f_{cls}^{tag})) \leq d_{\mathcal{H}}(p(\mathbf{z}|y; f_{cls}^{src}), p(\mathbf{z}|y; f_{cls}^{tag}))$ and the definition of induce image $\tilde{\mathcal{D}}$ of \mathcal{D} over \mathcal{R} , we have:

$$\begin{aligned}
 & d_{\mathcal{H}}(\tilde{\mathcal{D}}'_s, \tilde{\mathcal{D}}_t) \\
 &\leq \tau d_{\mathcal{H}}(\tilde{\mathcal{D}}_s, \tilde{\mathcal{D}}_t) + (1 - \tau) d_{\mathcal{H}}(\tilde{\mathcal{D}}_G, \tilde{\mathcal{D}}_t) \\
 &\leq \tau d_{\mathcal{H}}(\tilde{\mathcal{D}}_s, \tilde{\mathcal{D}}_t) + (1 - \tau) d_{\mathcal{H}}(\tilde{\mathcal{D}}_s, \tilde{\mathcal{D}}_t) = d_{\mathcal{H}}(\tilde{\mathcal{D}}_s, \tilde{\mathcal{D}}_t)
 \end{aligned} \tag{17}$$

Clearly, if Assumption 4.1 holds with $m > \frac{1}{2}d$, we can prove that $J(m', d) < j(m, d)$ and $d_{\mathcal{H}}(\tilde{\mathcal{D}}'_s, \tilde{\mathcal{D}}_t) < d_{\mathcal{H}}(\tilde{\mathcal{D}}_s, \tilde{\mathcal{D}}_t)$. Furthermore, it can easily be seen that $\epsilon_{S'}(h) < \epsilon_S(h)$ and $\min(\epsilon_{\mathcal{T}}(h) + \epsilon_{S'}(h)) < \min(\epsilon_{\mathcal{T}}(h) + \epsilon_S(h))$ if $(\epsilon_S(h) - \epsilon_{S'}(h)) > 0$ is bounded. Combining Eq. (14), it is now obvious that:

$$\begin{aligned}
 \epsilon_{\mathcal{T}}(h) &\leq \hat{\epsilon}_{S'}(h) + J(m', d) + d_{\mathcal{H}}(\tilde{\mathcal{D}}'_s, \tilde{\mathcal{D}}_t) + \lambda' \\
 &\leq \hat{\epsilon}_S(h) + J(m, d) + d_{\mathcal{H}}(\tilde{\mathcal{D}}_s, \tilde{\mathcal{D}}_t) + \lambda
 \end{aligned} \tag{18}$$

This completes the proof. \square